*Polish Journal of Chemical Technology, 17, **1**, 11 — 17, 10.1515/pjct-2015-0003*

The effect of preparation method on the performance of $PtSn/Al_2O_3$ catalysts for acetic acid hydrogenation

Ke Zhang, Haitao Zhang, Hongfang Ma, Weiyong Ying*, Dingye Fang

East China University of Science and Technology, Engineering Research Center of Large Scale Reactor Engineering and Technology of the Ministry of Education, State Key Laboratory of Chemical Engineering, Shanghai 200237, China
**Corresponding author: e-mail: wying@ecust.edu.cn*

$PtSn/Al_2O_3$ catalysts with a given loading of 1 wt% Pt and 1 wt% Sn were prepared by co-impregnation or successive impregnation with aqueous solutions of Pt, Sn precursors and a commercial alumina. The catalysts were characterized by N_2 adsorption, H_2-TPR (H_2 temperature-programmed reduction), H_2-pulse chemisorption, XPS (X-ray photoelectron spectroscopy) and CO-FTIR (Fourier transform infrared spectroscopy), and tested in the hydrogenation of acetic acid. The results showed that the preparation method affected both the chemical properties and their performance in the hydrogenation of acetic acid. Sn enrichment on the catalysts surface was observed on the co-impregnated catalyst and catalyst in which the Pt precursor had been loaded first. It was found that the modification of Pt was a function of the sequence of Sn addition as revealed by CO-FTIR. Co-impregnated catalyst showed the highest activity and ethanol selectivity.

Keywords: PtSn catalysts, preparation method, acetic acid hydrogenation, XPS, CO-FTIR.

INTRODUCTION

The hydrogenation of acetic acid to ethanol is a reaction of industrial importance because the world is in great demand of gasoline and many countries are determined to promote the development of gasohol. Ethanol is mainly produced by means of ethylene hydration and fermentation and both routes have some problems[1]. The former process depends on petroleum industry and doesn't suit for countries that are poor in oil while the latter one can't be applied to countries with limited arable land because it consumes large quantity of crops and food. What's more, the production of fuel-grade ethanol is expensive and energy-inefficient because both processes involve energy-intensive distillation steps. On the other hand, acetic acid is readily available since the homogeneous methanol carbonylation technology developed by Monsanto exhibited high activity and selectivity under mild operating conditions[2]. Traditionally, CO and H_2 used in methanol synthesis and carbonylation are mainly produced by catalytic partial oxidation or steam-reforming of light hydrocarbons from petroleum[3–6]. Furthermore, syngas was obtained from coal gasification[7, 8].

The information in open literature regarding acetic acid hydrogenation is limited. Copper chromite catalysts have been widely used in various industrial processes such as the hydrogenation of vegetable oils, esters and fatty acids[9–11]. Reports on Cr free Cu catalysts for acetic acid hydrogenation are also available[12, 13]. A series of experiments were carried out by Pestman et al. to explore the oxidation of carboxylic acids (acetic acid included) on oxides obtaining acetones and aldehydes[14–16]. Rachmady and Vannice carried out experiments on the hydrogenation of acetic acid on Pt catalysts supported on oxides and revealed that Pt supported on TiO_2 is a promising catalyst for acetic acid hydrogenation to ethanol obtaining 50% ethanol, 30% ethyl acetate and 20% ethane[17, 18]. Later, Alcala indicated that the addition of Sn to Pt/SiO_2 can avoid the cleavage of C-C bond in acetic acid and promote the selective conversion of acetic acid to ethanol, acetaldehyde, and ethyl acetate[19].

Bimetallic PtSn catalysts on various supports are widely used in many processes, such as reforming[20] and dehydrogenation of hydrocarbons[21–23] for the petroleum industry and the selective hydrogenations in fine chemistry[24–28] because they usually show better performance in terms of activity, selectivity and/or stability, than monometallic platinum catalysts. For instance, the addition of Sn to Pt altered the selectivity in naphtha reforming, reducing the catalyst deactivation caused by coke deposition[29]. It has been found that the methodology adopted in the preparation of PtSn catalysts can result in different metallic phases, and plays a crucial role in determining the properties of the sample and its catalytic performance[26, 27, 30, 31]. The accurate nature of PtSn systems are very complicated and still a matter of debate, and different techniques like TPR, FT-IR, XRD, and XPS were adopted to characterize the metallic structures of these bimetallic catalysts[26–30]. For example, by using XPS, alloys formation between Pt and Sn was observed by Morales et al. in the co-impregnated samples, while in the sequentially impregnated catalysts (load Pt to Sn/H[Al]ZSM5) no alloy was formed but the reduction of the two metals were much more easy[31]. In another study, XPS and CO-FTIR were used to investigated the nature of several TiO_2 supported PtSn catalysts revealing that the catalysts prepared by co-impregnation showed better performance for the gas phase hydrogenation of crotonaldehyde due to the presence of decorated Pt species[32]. The preparation of $PtSn/Al_2O_3$ catalysts using controlled surface reaction techniques can also improve the catalytic behavior in butane dehydrogenation, i.e. inhibiting cracking and coke formation reactions, as well as enhance the stability of the catalyst[21, 22].

Our previous study has demonstrated that co-impregnated $PtSn/Al_2O_3$ catalysts showed better performance in the hydrogenation of acetic acid to ethanol, as compared to monometallic Pt catalyst, and an appropriate Sn/Pt ratio was evidentiated. In this paper, $PtSn/Al_2O_3$ catalysts were prepared by co-impregnation and successive impregnation and characterized by N_2 adsorption, TPR, XPS and CO-FTIR as well as tested in acetic acid hydrogenation.

EXPERIMENTAL PART

Catalyst preparation

Three bimetallic PtSn catalysts with the same loading (1.0 wt% Pt, 1.0 wt% Sn) were prepared by co-impregnation and successive impregnation. Hexachloroplatinic (IV) acid hexahydrate, tin (IV) chloride pentahydrate and aluminum oxide activated (purchased from Sinopharm Chemical Reagent Co., Ltd) were used as Pt, Sn precursors and support. Before impregnation, the support was ground and sieved to 40–60 mesh and calcined (550°C, 12 h) to remove the organic contaminants. For the co-impregnated catalyst [1Pt1Sn-C], appropriate amount of $H_2PtCl_6 \cdot 6H_2O$ and $SnC1_4 \cdot 5H_2O$ were dissolved in deionized water to obtain a homogeneous solution; then the solution was added dropwise to the calcined support (1 ml soln $\cdot$ g^{-1} Al_2O_3), which was aged for 12 h at ambient temperature. The catalyst was dried in an oven at 120°C overnight in air and then calcined at 550°C for 12 h. Another catalyst [1Pt1Sn-S1] was prepared by impregnation of monometallic Pt catalyst with aqueous $SnC1_4 \cdot 5H_2O$ solution and then dried and calcined as described above, whereas the monometallic Pt catalyst was subjected to the same procedure even if the impregnation solution only contains $H_2PtCl_6 \cdot 6H_2O$. Another catalyst [1Pt1Sn-S2] was prepared by successive impregnation, but reversing the order of precursor addition (first introducing $SnC1_4 \cdot 5H_2O$).

Catalyst characterization

The BET (Brunauer Emmett Teller) surface area, average pore diameter, and pore size distribution of the catalysts and the support were determined by means of nitrogen physisorption using a Micromeritics ASAP 2020 M automated system.

H_2-TPR was performed on a Micromeritics AutoChem II 2920 system. Generally, 0.20 g sample was placed in a quartz U-tube reactor and calcined at 500°C for 1 h under Ar (99.99%) atmosphere and then cooled down to room temperature. The reductive mixture (10% H_2 in Ar) was fed to the reactor at a flow rate of 50 ml $\cdot$ min^{-1}. The TPR experiments were carried out from room temperature to 700°C with a ramp of 10°C $\cdot$ min^{-1} and the hydrogen consumption were monitored by a thermal conductivity detector (TCD) after the base line was stable.

The active sites and dispersion of the catalysts were determined by H_2-pulse chemisorption technique using the same system as adopted in TPR. The samples were reduced under H_2 (99.99%, 30 ml $\cdot$ min^1) at 350°C for 2 h, then purged in He (99.99%, 30 ml $\cdot$ min^{-1}) at 350°C for 1.5 h and then cooled down to room temperature in flux of He (30 ml $\cdot$ min^{-1}). Calibrated pulses of H_2 were injected into the system repeatedly and the time between pulses was 4 min until no further H_2 consumption was observed. Photoelectron spectra were recorded over calcined and reduced samples (350°C, 2 h) using an ESCALAB 250Xi (Thermo Fisher, USA) photoelectron spectrometer coupled with an Al Kα X-ray operated at 10 mA and 12 kV. The energy regions of the photoelectrons of interest were repeatedly scanned to get good signal-to-noise ratios. The intensity of the peaks were quantified by determining the integral of each peak after subtracting an S-shaped background and fitting the experimental peaks to Lorentzian/Gaussian lines (80% L/20% G). The C1s line was taken as an internal standard at 284.8 eV.

CO-FTIR was carried out in a spectrometer (Nicolet 6700, Thermo, USA) which had been modified to allow in situ catalyst pretreatment. The infrared cell was equipped with temperature controlled parts and a ZnSe window. Infrared spectra of adsorbed species were collected at atmospheric pressure and room temperature at a resolution of 4 cm^{-1}. The catalysts (0.03 g, 180 mesh) were reduced in situ for 2 h under atmospheric pressure by hydrogen at 350°C (30 ml $\cdot$ min^{-1}, 5°C $\cdot$ min^{-1}) and purged with pure nitrogen (99.99%) for 1 h at 350°C. CO was introduced into the DRIFT cell until saturation after cooling the samples to room temperature in a N_2 flow.

Activity testing

The hydrogenation of acetic acid (99.95%, Sinopharm Chemical Reagent Co., Ltd, China) was carried out in a fixed-bed reactor with an inner diameter of 10 mm. Approximately 2.5 g catalyst was loaded in the isothermal region of the reactor. Prior to the experiments, the catalysts were reduced in flowing H_2 (100 ml $\cdot$ min^{-1}) at 350°C for 2 h. Acetic acid was vaporized by preheating and carried by H_2 flux into the reactor. The effluent was monitored after passing through the condenser and the liquid-vapor seperator. Agilent 7890A GC with a thermal conductivity detector (TCD) and a flame ionization detector (FID) was used to analyze the products. Compositions of the tail gas were determined on-line and the products in the liquid phase were detected off-line. The TCD was equipped with a molecular sieve 5A packed column and a Hayesep Q packed column while the FID was coupled with an HP-PLOT/Q capillary column and an HP-INNOWAX capillary column. Finally, the acetic acid in the liquid was determined by titration.

RESULTS AND DISCUSSION

N_2 adsorption

Table 1 shows data on the textural property of the catalysts and the support. The introduction of metals caused a loss of surface area and a slight increase in average pore diameter, which resulted from the blocking of the pores of Al_2O_3. It is worth noting that the pore distribution behavior of the catalysts was affected by the impregnation procedure, as vividly shown in Figure 1. For catalysts 1Pt1Sn-S1 and 1Pt1Sn-S2 the distribution of pores smaller than 8 nm decreased while the pores distributed between 8–32 nm bore a little increase, compared to Al_2O_3. On the other hand, changes of pore distribution on 1Pt1Sn-C showed in pores about 7–13 nm. This phenomenon is probably due to the fact that a reaction between both metallic precursors in the impregnating solution would lead to a high concentration of a PtSn complex[33] that didn't exist in the sequence-impregnated catalysts or due to the different interactions taking place between the metallic precursors and the alumina support in the initial stages of the catalyst preparation procedure.

Table 1. The results of N_2 adsorption and H_2-pulse chemisorption

Sample	S_{BET} [$m^2 \cdot g^{-1}$]	Volume of the pore [$cm^3 \cdot g^{-1}$]	Average pore diameter [nm]	H/Pt	$H_{chem.}$ [$\mu mol \cdot g^{-1}_{cat.}$]
1Pt1Sn-C	162.9	0.45	11.0	0.30	15.33
1Pt1Sn-S1	171.9	0.46	10.8	0.37	19.17
1Pt1Sn-S2	179.5	0.47	10.5	0.40	20.75
Al_2O_3	221.8	0.46	8.3	–	–

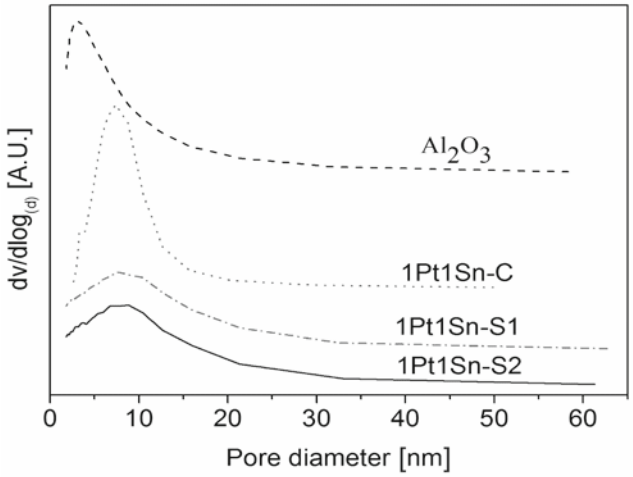

Figure 1. The distribution of pore diameter of the catalysts and support

H_2-TPR

The TPR profile of the catalysts is shown in Figure 2. On 1Pt1Sn-C, only one peak appeared between 200–300°C, which was due to the co-reduction of Pt and Sn[34]. Both the sequential impregnated catalysts showed a distinct reduction peak centered at about 120°C along with a shoulder located between 200–300°C. The peak in the lower temperature range can be ascribed to the reduction of unalloyed Pt in weak interaction with the support[35]. Our previous experiment indicated that Sn/Al_2O_3 consumed H_2 over a wide temperature range (from 200–700°C) with a maximum at about 480°C while the reduction peak of monometallic Pt/Al_2O_3 centered at about 240°C [34]. Thus, the shoulder between 200–300°C can be ascribed to the reduction of Pt in strong interaction with alumina or the co-reduction of Pt and Sn[35, 36]. Furthermore, a minor peak centered at 450°C emerged on 1Pt1Sn-S2, which is attributed to the reduction of isolated Sn species[34].

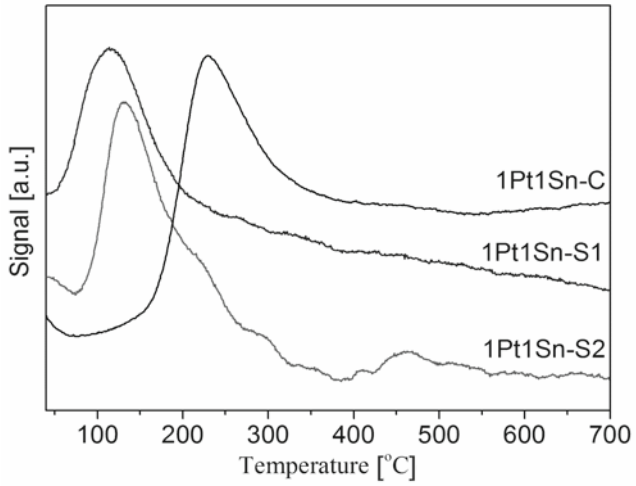

Figure 2. The TPR profiles of the catalysts

H_2-pulse chemisorption

The amount of hydrogen irreversibly adsorbed at 25°C on the reduced samples was summarized in Table 1. Compared to monometallic Pt/Al_2O_3 catalyst (1Pt)[34], the chemisorption capacity of hydrogen on the catalysts all decreased dramatically and influenced by the preparation procedure adopted, as the H/Pt ratio increased from 0.30 for 1Pt1Sn-C to 0.37 for 1Pt1Sn-S2 to 0.40 for 1Pt1Sn-S1. The relative lower H/Pt ratio of the co-impregnated catalyst may caused by the reaction between both metallic precursors in the impregnating solution which would lead to a high concentration of a PtSn complex[33], and the covering of Pt by Sn species was more prominent on the reduced catalysts due to the intimate contact between Pt and Sn.

XPS

XPS experiments were carried out to determinate the chemical state of Pt, Sn in the fresh and reduced (H_2, 350°C 2 h) catalysts. Pt 4d lines were analyzed instead of Pt 4f because the energy region of Pt 4f was overlapped by the intense Al 2p peak. XPS results showed that platinum was completely reduced in all the samples studied, because the Pt $4d_{5/2}$ spectra (omitted for brief) contained only one peak centered around 315 eV. Figure 3 shows the Sn $3d_{5/2}$ spectra of both fresh and reduced catalysts. After deconvolution, the Sn $3d_{5/2}$ spectrum of the fresh catalysts can be divided into two peaks: one with a low binding energy at 486.5–486.8 eV, and a second one at 487.6–487.8 eV. According to the literature[26, 28], it is not possible to discriminate between Sn^{II} or Sn^{IV} species, thus both of the two components were assigned to oxidized tin (Sn^{II} or Sn^{IV}), probably forming chlorinated species[25, 29]. When the catalysts were reduced, a new peak at 485.5–485.7 eV emerged, which can be ascribed to metallic Sn[30].

The quantitative result of XPS analysis was present in Table 2. The Sn/Pt ratio of the catalysts (both fresh and reduced) were much higher than the bulk one (1.22), which is indicative of Sn enrichment on the surface of the catalyst, as revealed by others[32]. It is worth mentioning that the Sn/Pt ratio of 1Pt1Sn-C and 1Pt1Sn-S1 increased substantially after reduction. This increase can be assigned to 2 main effects: (i) dilution of platinum by metallic tin, upon the formation of PtSn bimetallic phases, (ii) covering of Pt metal particle surface by oxidized tin species.

CO-FTIR

The interactions between Pt and Sn should change the electronic environment of Pt atoms. The electronic state of the surface platinum atoms was characterized by CO probe molecules via adsorption. The IR spectra of CO chemisorbed on the reduced catalysts were shown in Figure 4. Generally, the bands in the frequency region of 1950–2100 cm^{-1} were related to CO linearly bonded

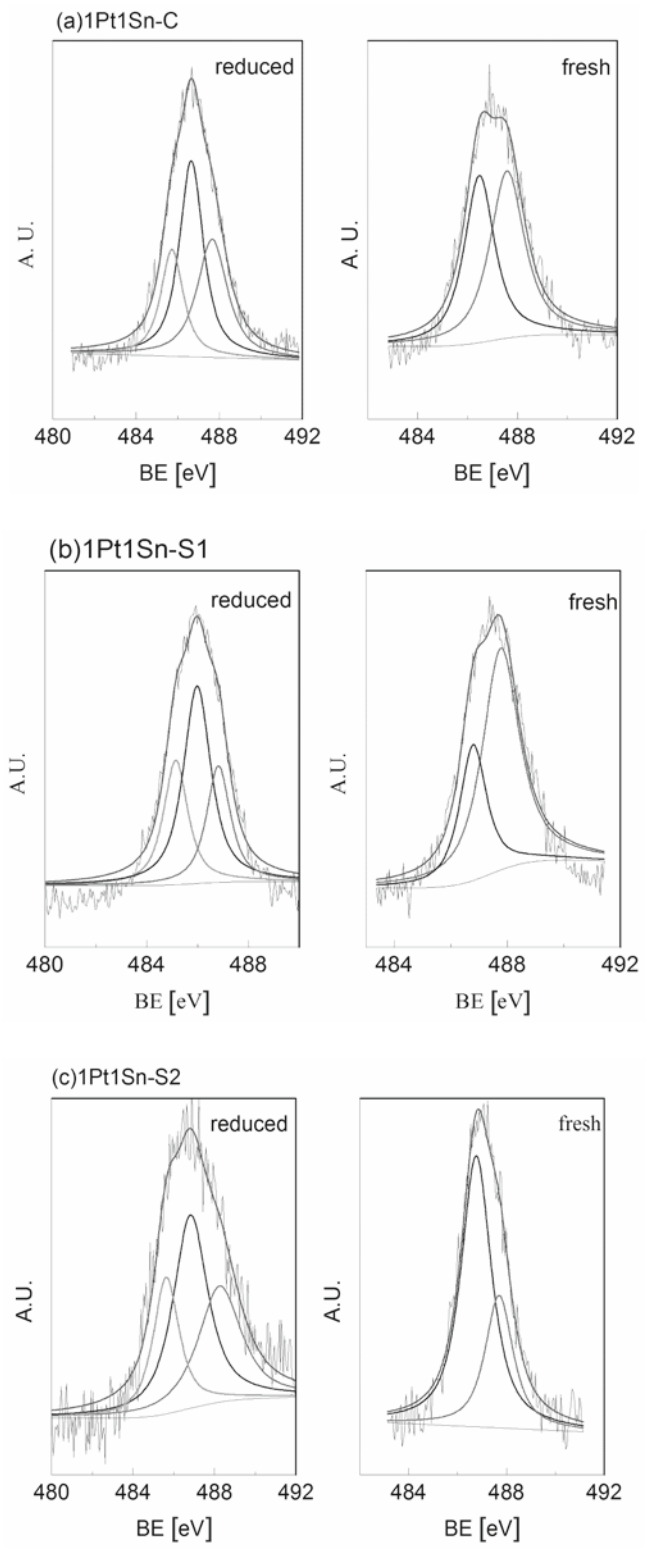

Figure 3. The $3d_{5/2}$ spectrum of the fresh and reduced catalysts

to one surface-exposed metal Pt atom while the band centered at about 1830 cm^{-1} was assigned to CO bonded to two surface Pt atoms (bridged species)[37–40]. On monometallic Pt catalyst, the spectrum showed a main peak at 2063 cm^{-1} along with a shoulder at 2080 cm^{-1}, as well as a minor peak located at about 1818 cm^{-1}. The introduction of Sn lead to different observations, depending on the preparation procedure. On one hand, the shoulder at 2080 cm^{-1} disappeared on all the bimetallic catalysts and the minor peak at 1818 cm^{-1} became invisible on 1Pt1Sn-C and 1Pt1Sn-S1. On the other hand, a broadening of the main peak at 2063 cm^{-1} occurred on 1Pt1Sn-S2. Furthermore, a new peak even emerged in the frequency region of 1950–2050 cm^{-1} on 1Pt1Sn-C and 1Pt1Sn-S1.

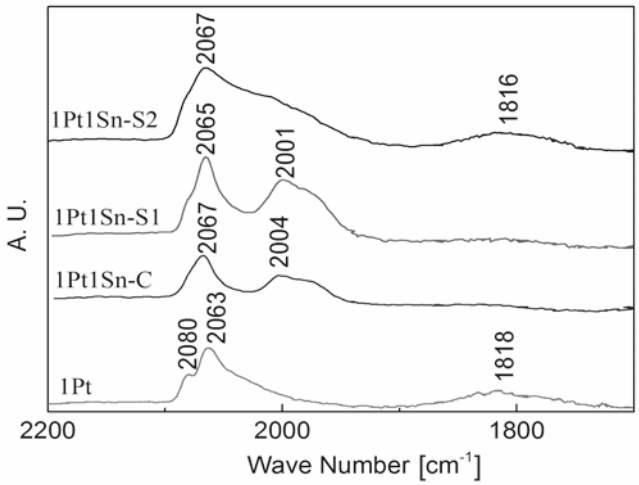

Figure 4. CO-FTIR spectrum of the catalysts

In a previous study[39], Arteaga et al. reported that the positions of bands due to linearly adsorbed CO on Pt were a function of Pt dispersion: the shoulder at 2080 cm^{-1} was related to large ensembles of Pt atoms akin to exposed low-index planes (big ensembles), bands at 2060–2067 cm^{-1} ascribed to highly coordinated Pt atoms in medium-sized ensembles of Pt atoms, and the bands located at < 2030 cm^{-1} assigned to the lowest coordination sites, which were probably corner or apex atoms on small Pt particles. Thus, the spectra indicated that the Pt distribution was apparently heterogeneous on monometallic Pt catalyst and the introduction of Sn changed the dispersion of Pt. According to Riguetto et al.[40], the asymmetry of the main band as well as its broadening on the low-frequency side of 1Pt1Sn-S2 was indicative of the presence of CO bonded to the steps, and the absence of the peak at about 1816 cm^{-1} on 1Pt1Sn-C and 1Pt1Sn-S1 meant a more homogeneous distribution of steps or corner sites present on the surface[40]. Con-

Table 2. The quantitative results of XPS of the fresh and reduced catalysts

Sample	Atom ratio					BE [eV]	
	Pt/Al	Sn/Al	Sn/Pt	Pt		Sn	
1Pt1Sn-C	0.0038	0.0076	2.0	317.2 (100%)	–	486.5 (47%)	487.6 (53.0)
[1]1Pt1Sn-C	0.0025	0.0096	3.7	315.0 (100%)	485.7 (22%)	486.6 (44%)	487.6 (34%)
1Pt1Sn-S1	0.0035	0.0085	2.4	317.0 (100%)	–	486.8 (31%)	487.8 (69%)
[1]1Pt1Sn-S1	0.0026	0.010	4.0	314.8 (100%)	485.6 (27%)	486.5 (48%)	487.3 (25%)
1Pt1Sn-S2	0.003	0.0061	2.0	316.9 (100%)	–	486.7 (69%)	487.6 (31%)
[1]1Pt1Sn-S2	0.0029	0.0060	2.1	315.1 (100%)	485.5 (25%)	486.6 (43%)	488.0 (32%)

[1]Reduced catalyst.

cerning the result of Sn/Pt ratio revealed by XPS, the reason of this phenomenon is that part of the Pt surfaces were covered or decorated by Sn species, on 1Pt1Sn-C and 1Pt1Sn-S1, thus leading to the decrease of stepped Pt and the selectively poison of Pt sites responsible for the bridging CO.

Acetic acid hydrogenation

The hydrogenation of acetic acid was carried out at 275°C and 255°C while other conditions were fixed at 2.0 MPa LHSV = 0.96 L · $g^{-1}_{cat.}$ · h^{-1} and $n(H_2)/ n(CH_3CO\text{-}OH) = 10$. The evolution of catalytic activity (the conversion of acetic acid) as a function of time on stream at 275°C for the catalysts was plotted in Figure 5 and data were reported after a carbon balance (within ±5%) was achieved. The behavior was similar in all cases, the activity increased during the first 12 h, thereafter remaining practically stable as a function of time on stream. The conversion of acetic acid and production selectivity of the catalysts were listed in Table 3. The bimetallic catalysts were much more active than the monometallic one[34], and the catalyst prepared by co-impregnation showed the highest activity, following the order 1Pt1Sn-C > 1Pt1Sn-S1 ≈ 1Pt1Sn-S2, at both temperature. Taking into account the results of XPS and H_2-pulse chemisorption, co-impregnated catalyst showed the lowest Pt dispersion after reduction, which means that the remaining surface Pt atoms were much more active (because our previous study revealed that monometallic Sn catalysts almost showed no activity towards acetic acid hydrogenation)[34]. In addition, observable differences in product selectivity were also detected among the catalysts depending on the type of impregnation strategy employed. The selectivity of aldehyde and ethane were almost the same on all catalysts while the selectivity towards ethanol and ethyl acetate bore significant disparity. The result of CO-FTIR indicated that a part of Pt species on 1Pt1Sn-S2 was different from other two catalysts, which probably showed different desorption capacity of ethanol and lead to a higher selectivity to ethyl acetate. What's more, 1Pt1Sn-S2, which showed the lowest activity and selectivity to ethanol, also produced much more methane. The result of H_2-TPR indicated that there would be segregated Sn species on the surface of 1Pt1Sn-S2, which meant that the contact between Pt and Sn was less intimate and the decoration of Pt by Sn species on the reduced catalysts was less prominent. The study of Vilella et al. indicated that Sn addition to Pt/SiO_2 catalysts can form PtSn alloy and suppress the cleavage of C-C bond of acetic acid which lead to the production of methane[19]. Thus, this explanation can be also applied to our case.

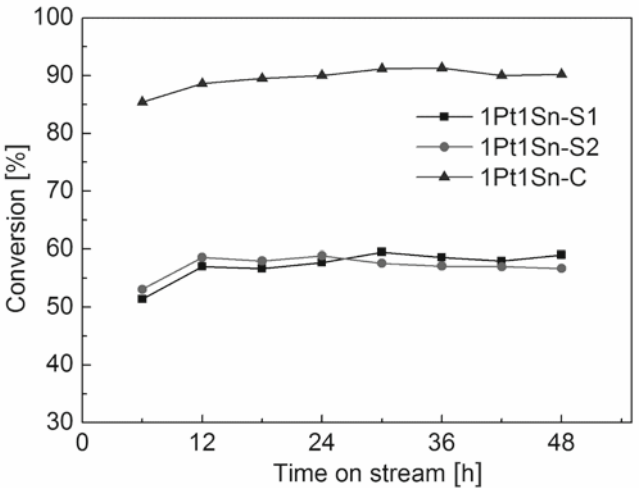

Figure 5. The evolution of catalytic activity as a function of time of the catalysts

CONCLUSIONS

Bimetallic PtSn catalysts supported on alumina have been prepared which were very active and selective to ethanol and ethyl acetate, in the vapor phase hydrogenation of acetic acid. H_2-TPR showed that the reduction of Pt was promoted in sequentially impregnated catalysts and the co-reduction of Pt and Sn was less obvious. Platinum dispersion decreased after Sn addition, which was due to surface covering of Sn species and/or to the formation of PtSn alloy. XPS measurement revealed the presence of Sn in both zero and oxidized states in the reduced catalysts, and the extent of Sn species enrichment on the catalysts surface depend on the preparation method used. The absence of Pt sites responsible for bridging CO on co-impregnated catalyst and catalyst loading first with Pt, as well as the broadening of the main peak on 1Pt1Sn-S2 demonstrated that different preparation methods can lead to diverse electronic and geometrical effects that can reduce the concentration of exposed Pt. PtSn catalyst prepared by co-impregnation showed the highest activity and selectivity to ethanol.

ACKNOWLEDGMENT

This work is financially supported by the National Science and Technology Supporting Plan (2006BAE02B02).

LITERATURE CITED

1. Velu, S. & Santosh, K.G. (2008). A review of recent literature to search for an efficient catalytic process for the conversion of syngas to ethanol. *Energ. Fuel. 22*, 814–839. DOI: 10.1021/ef700411x.

Table 3. The performance of the catalysts in acetic acid hydrogenation

Catalysts	Conversion [%]	Selectivity [%]				
		C_2H_6O	$C_4H_8O_2$	C_2H_4O	CH_4	C_2H_6
1Pt1Sn-C^H	90.0	58.5	35.1	1.8	3.1	1.4
1Pt1Sn-C^L	74.6	72.5	24.1	1.0	1.8	0.6
1Pt1Sn-S1^H	55.7	54.9	38.7	1.8	3.6	1.0
1Pt1Sn-S1^L	44.3	67.1	28.5	1.2	2.3	0.9
1Pt1Sn-S2^H	54.7	29.7	61.2	0.8	8.5	1.7
1Pt1Sn-S2^L	43.2	37.4	51.5	0.7	8.2	2.2

^{H}Operated at 275°C.

^{L}Operated at 250°C.

2. Yoneda, N., Kusano, S., Yasui, M., Pujad, P. & Wilcher, S. (2001). Recent advances in processes and catalysts for the production of acetic acid. *Appl. Catal. A: Gen.* 221, 253–265. DOI: 10.1016/S0926-860X (01) 00800-6.

3. Mahajan, S., Nickolas, Menzies, W.R. & Albrigh, L.F. (1977). Partial oxidation of light hydrocarbons. 1. Major differences noted in various tubular reactors. *Ind. Eng. Chem. Proc. Des. Dev.*, 1977, 16(3), 271–274. DOI: 10.1021/i260063a003.

4. Sidjabat, O. & Trimm, D.L. (2000). Nickel-magnesia catalysts for the steam reforming of light hydrocarbons. *Top. Catal.* 11–12(1–4), 279–282. DOI: 10.1023/A:1027212301077.

5. Mahajan, S., Nickolas, D.M., Sherwood, F., Menzies, W.R. & Albrigh, L.F. (1977). Partial oxidation of light hydrocarbons. 2. New techniques for investigating surface reactions. *Ind. Eng. Chem. Proc. Des. Dev.*, 16 (3): 275–278. DOI: 10.1021/i260063a0045.

6. Yarze, J.C. & Lockerbie, T.E. Catalytic steam reforming of light liquid hydrocarbons. http://web.anl.gov/PCS/acsfuel/preprint%20archive/Files/04_1_CLEVELAND_0460_0078.pdf

7. Van Dyk, J.C., Keyser, M.J. & Coertzen, M. (2006). Syngas production from South African coal sources using Sasol-Lurgi gasifiers. *Int. J. Coal Geol.* 65, 243–253. DOI: 10.1016/j.coal.2005.05.007.

8. Minchener, A.J. (2005). Coal gasification for advanced power generation. *Fuel* 84, 2222–2235. DOI: 10.1016/j.fuel.2005.08.035.

9. Aly, M. & Baumgarten, E. (2001). Hydrogenation of hexanoic acid with different catalysts. *Appl. Catal. A: Gen.* 210, 1–12. DOI: 10.1016/S0926-860X(00)00791-2.

10. Turek, T., Trim D.L. & Cant, N.W. (1994). The Catalytic hydrogenolysis of esters to alcohols. *Catal. Rev.* 36(4), 645–683. DOI: 10.1080/01614949408013931.

11. Rao, R., Dandekar, A., Baker, R.T.K. & Vannice, M.A. (1997). Properties of copper chromite catalysts in hydrogenation reactions. *J. Catal.* 171, 406–419. DOI: 10.1006/jcat.1997.1832.

12. Natal Santiago, M.A., Sánchez-Castillo, M.A., Cortright, R.D. & Dumesic, J.A. (2000). Catalytic reduction of acetic acid, methyl acetate, and ethyl acetate over silica-supported copper. *J. Catal.* 193, 16–28. DOI:10.1006/jcat.2000.2883.

13. Onyestyáka, G., Szabolcs Harnosa, S., Klébert, S., Stolcová, M., Kaszonyi, A. & Kalló, D. (2013). Selective reduction of acetic acid to ethanol over novel Cu_2In/Al_2O_3 catalyst. *Appl. Catal. A: Gen.* 464–465, 313–321. DOI:1 0.1016/j.apcata.2013.05.042.

14. Pestman, R., Koster, R.M., Boellaard, E., van derKraan, A.M. & Ponec, V. (1998). Identification of the active sites in the selective hydrogenation of acetic acid to acetaldehyde on iron oxide catalysts. *J. Catal.* 174, 142–152. DOI: 0021-9517/98.

15. Pestman, R., van Duijne, A., Pieterse, J.A.Z. & Ponec, V. (1995). The formation of ketones and aldehydes from carboxylic acids, structure-activity relationship for two competitive reactions. *J. Mol. Catal. A: Chem.* 103, 175–l80. DOI: 1381–1169/95.

16. Pestman, R., Koster, R.M., Pieterse, J.A.Z. & Ponec, V. (1997). Reactions of carboxylic acids on oxides: 1. Selective hydrogenation of acetic acid to acetaldehyde. *J. Catal.* 168, 255–264. DOI: 10.1006/jcat.1997.1623.

17. Rachmady, W. & Vannice, M.A. (2000). Acetic acid hydrogenation over supported platinum catalysts. *J. Catal.* 192, 322–334. DOI: 10.1006/jcat.2000.286.

18. Rachmady, W. & Vannice, M.A. (2002). Acetic acid reduction by H_2 over supported Pt catalysts: A DRIFTS and TPD/TPR study. *J. Catal.* 207, 317–330. DOI: 10.1006/jcat.2002.3556.

19. Alcala, R., Shabaker, J.W., Huber, G.W., Sanchez-Castillo, M.A. & Dumesic, J.A. (2005). Experimental and DFT studies of the conversion of ethanol and acetic acid on PtSn-based catalysts. *J. Phys. Chem. B.* 109, 2074–2085. DOI: 10.1021/jp049354t.

20. Hoang, D.L., Farrage, S.A-F., Radnik, J., Pohl, M-M., Schneider, M., Lieske, H. & Martin, A. (2007). A comparative study of zirconia and alumina supported Pt and Pt-Sn catalysts used for dehydrocyclization of *n*-octane. *Appl. Catal. A: Gen.* 333, 67–77. DOI: 10.1016/j.apcata.2007.09.003.

21. Siri, G.J., Ramallo-Lópezc, J.M., Casella, M.L., Fierrod, J.L.G., Requejo, F.G. & Ferretti, O.A. (2005). XPS and EXAFS study of supported PtSn catalysts obtained by surface organometallic chemistry on metals: Application to the isobutane dehydrogenation. *Appl. Catal. A: Gen.* 278, 239–249. DOI: 10.1016/j.apcata.2004.10.004.

22. Bocanegra, S.A., de Miguel, S.R., Borbath, I., Margitfalvi, J.L. & Scelza, O.A. (2009). Behavior of bimetallic $PtSn/Al_2O_3$ catalysts prepared by controlled surface reactions in the selective dehydrogenation of butane. *J. Mol. Catal. A: Chem.* 301, 52–60. DOI: 10.1016/j.molcata.2008.11.006.

23. de Miguel, S.R., Bocanegra, S.A., Julieta Vilella, I.M., Guerrero-Ruiz, A. & Scelza, O.A. (2007). Characterization and catalytic performance of PtSn catalysts supported on Al_2O_3 and Na-doped Al_2O_3in n-butane dehydrogenation. *Catal. Lett.* 119, 5–15. DOI: 10.1007/s10562-007-9215-5.

24. de Miguel, S.R., Román-Marínez, M.C., Jablonski, E.L., Fierro, J.L.G., Cazorla-Amorós, D. & Scelza, O.A. (1999). Characterization of bimetallic PtSn catalysts supported on purified and H_2O_2-functionalized carbons used for hydrogenation reactions. *J. Catal.* 184, 514–525. DOI: 10.1006/jcat.1999.2457.

25. Coloma, F., Sepfilveda-Escribano, A., Fierro, J.L.G. & Rodriguez-Reinoso, F. (1996). Crotonaldehyde hydrogenation over bimetallic Pt-Sn catalysts supported on pregraphitized carbon black: Effect of the Sn/Pt atomic ratio. *Appl. Catal. A: Gen.* 136, 231–248. DOI: 10.1016/0926-860X(95)00259-6.

26. Coloma, F., Sepfilveda-Escribano, A., Fierro, J.L.G. & Rodriguez-Reinoso, F. (1996). Crotonaldehyde hydrogenation over bimetallic Pt-Sn catalysts supported on pregraphitized carbon black: Effect of the preparation method. *Appl. Catal. A: Gen.* 148, 63–80. DOI: 10.1016/S0926-860X(96)00218-9.

27. Homs, N., Llorca, J., de la Piscina, P.R., Francisco Rodríguez-Reinoso, F., Sepúlveda-Escribano, A. & Silvestre-Albero, J. (2001). Vapour phase hydrogenation of crotonaldehyde over magnesia-supported platinum tin catalysts. *Phys. Chem. Chem. Phys.* 3, 1782–1788. DOI: 10.1039/b100770j.

28. Vilella, I.M.J., de Miguel, S.R., de Lecea, C.S-M., Linares-Solano, Á. & Scelza, O.A. (2005). Catalytic performance in citral hydrogenation and characterization of PtSn catalysts supported on activated carbon felt and powder. *Appl. Catal. A: Gen.* 281, 247–258. DOI: 10.1016/j.apcata.2004.11.034.

29. Vu, B.K., Song, M.B., Ahn, I.Y., Suh, Y-W., Suh, D.J., Kim, W-I., Koh, H-L., Choi, Y.G. & Shin, E.W. (2011). Pt-Sn alloy phases and coke mobility over $Pt-Sn/Al_2O_3$ and $Pt-Sn/ZnAl_2O_4$ catalysts for propane dehydrogenation. *Appl. Catal. A: Gen.* 400, 25–33. DOI: 10.1016/j.apcata.2011.03.057.

30. Ricardo, M., Luis, M., Aura, L. & Francisco, Z. (2005). Characterization of bifunctional PtSn/H[Al]ZSM5 catalysts: a comparison between two impregnation strategies. *J. Mol. Catal. A: Chem.* 228, 227–232. DOI: 10.1016/j.molcata.2004.09.036.

31. Pakornphant, C., Sumaeth, C. & Johannes, S. (2004). Temperature-programmed desorption of methanol and oxidation of methanol on $Pt-Sn/Al_2O_3$ catalysts. *J. Chem. Eng.* 97, 161–171. DOI: 10.1016/S1385-8947(03)00178-5.

32. Ruiz-Martínez, J., Sepúlveda-Escribano, A., Anderson, J.A. & Rodríguez-Reinoso, F. (2007). Influence of the preparation method on the catalytic behavior of $PtSn/TiO_2$ catalysts. *Catal. Today.* 123, 235–244. DOI: 10.1016/j.cattod.2007.02.013.

33. Luciene, S.C., Patricio, R., Gina, P., Nora, F., Carlos, L.P. & Maria do, C.R. (2001). Effect of the solvent used during preparation on the properties of Pt/Al_2O_3 and $Pt-Sn/Al_2O_3$ catalysts. *Ind. Eng. Chem. Res.* 40, 5557–5563. DOI: 10.1021/ie000939t.

34. Zhang, K., Zhang, H.T., Ma, H.F., Ying, W.Y. & Fang, D.Y. (2014). Effect of Sn addition in gas phase hydrogenation of acetic acid on alumina supported PtSn catalysts. *Catal. Lett.* 144, 691–701. DOI: 10.1007/s10562-014-1210-z.

35. Armendáriz, H., Guzmán. A., Toledo, J.A., Llanos, M.E., Vázquez, A. & Aguilar-Ríos, G. (2001). Isopentane dehydrogenation on Pt-Sn catalysts supported on Al-Mg-O mixed oxides: effect of Al/Mg atomic ratio. *Appl. Catal. A: Gen.* 211, 69–80. DOI: 10.1016/S0926-860X(00)00836-X.

36. Ballarini, A.D., de Miguel, S.R., Castro, A.A. & Scelza, O.A. (2013). *n*-Decane dehydrogenation on Pt, PtSn and PtGe supported on pinels prepared by different methods of synthesis. *Appl. Catal. A: Gen.* 467, 235–245. DOI: 10.1016/j.apcata.2013.07.03.

37. Margitfalvi, J.L., Tompos, A., Kolosova, I. & Valyon, J. (1998). Reaction induced selectivity improvement in the hydrogenation of crotonaldehyde over Sn-Pt/SiO_2 catalysts. *J. Catal.* 174, 246–249. DOI: 0021-9517/98.

38. Yu, C.L., Ge, Q.J., Xu, H.Y. & Li, W.Z. (2006). Effects of Ce addition on the Pt-Sn/γ-Al_2O_3 catalyst for propane dehydrogenation to propylene. *Appl. Catal. A: Gen.* 315, 58–67. DOI: 10.1016/j.apcata.2006.08.038.

39. Arteaga, G.J., Anderson, J.A. & Rochester, C.H. (1999). FTIR study of CO adsorption on coked Pt-Sn/Al_2O_3 catalysts. *Catal. Lett.* 58, 189–194. DOI: 10.1023/A: 1019023210896.

40. Riguetto, B.A., Damyanova, S., Gouliev, G., Marques, C.M.P., Petrov, L. & Bueno, J.M.C. (2004). Surface behavior of alumina-supported Pt catalysts modified with cerium as revealed by X-ray diffraction, X-ray photoelectron spectroscopy, and Fourier transform infrared spectroscopy of CO adsorption. *J. Phys. Chem. B.* 108, 5349–5358. DOI: 10.1021/jp031167s.